Molecular Pharmacology Fast Forward. Published on September 12, 2019 as DOI: 10.1124/mol.119.115964
This article has not been copyedited and formatted. The final version may differ from this version.

A High-Throughput Screen of a Library of Therapeutics Identifies Cytotoxic Substrates of P-glycoprotein

Tobie D. Lee, Olivia W. Lee, Kyle R. Brimacombe, Lu Chen, Rajarshi Guha, Sabrina Lusvarghi, Bethilehem G. Tebase, Carleen Klumpp-Thomas, Robert W. Robey, Suresh V. Ambudkar, Min Shen, Michael M. Gottesman, Matthew D. Hall

National Center for Advancing Translational Sciences (T.D.L., O.W.L, K.R.B, L.C., R.G., C.K.-T., M.S., M.D.H.) National Institutes of Health, Rockville MD and [2]Laboratory of Cell Biology (S.L., B.G.T., R.W.R, S.V.A., M.M.G.), National Cancer Institute, National Institutes of Health, Bethesda, MD, U.S.A.

Molecular Pharmacology Fast Forward. Published on September 12, 2019 as DOI: 10.1124/mol.119.115964
This article has not been copyedited and formatted. The final version may differ from this version.

Running title: High-throughput screen to identify P-gp substrates

Corresponding Author:

Matthew D. Hall, PhD
National Center for Advancing Translational Sciences
National Institutes of Health
9800 Medical Center Drive, Building B
Rockville, MD 20850
hallma@mail.nih.gov

Number of text pages: 28

Number of tables: 2

Figures: 6

References: 46

Number of words in the Abstract: 250

Introduction: 687

Discussion: 912

Non-standard abbreviations:

P-gp, P-glycoprotein; BBB, blood-brain barrier; HTS, high-throughput screen; ABCB1, ATP-binding cassette family member B1; ABCG2, ATP-binding cassette family member G2; NCATS, National Center for Advancing Translational Science; NPC, NCATS Pharmaceutical Collection; MIPE, Mechanism Interrogation Plate; NPACT, NCATS Pharmacologically Active Chemical Toolbox; PhA, pheophorbide A; FTC, Fumitremorgin C; AUC, area under the curve; NAMPT, nicotinamide phosphoribosyltransferase; CDK, cyclin-dependent kinase; CRC, concentration-response curve; PI3K, phosphoinositide-3 kinase; mTOR, mammalian target of rapamycin; JAK, Janus kinase

Molecular Pharmacology Fast Forward. Published on September 12, 2019 as DOI: 10.1124/mol.119.115964
This article has not been copyedited and formatted. The final version may differ from this version.

Abstract

The ATP-binding cassette transporter P-glycoprotein (P-gp) is known to limit both brain penetration and oral bioavailability of many chemotherapy drugs. Although Food and Drug Administration guidelines require that potential interactions of investigational drugs with P-gp be explored, often this information does not enter into the literature. As such, we developed a high-throughput screen (HTS) to identify substrates of P-gp from a series of chemical libraries, testing a total of 10,804 compounds, most of which have known mechanisms of action. We used the CellTiter-Glo viability assay to test library compounds against parental KB-3-1 human cervical adenocarcinoma cells and the colchicine-selected sub-line KB-8-5-11 that over-expresses P-gp. KB-8-5-11 cells were also tested in the presence of a P-gp inhibitor (tariquidar) to assess reversability of transporter-mediated resistance. Of the tested compounds, a total of 90 P-gp substrates were identified including 55 newly identified P-gp substrates. Substrates were confirmed using an orthogonal killing assay against HEK-293 cells overexpressing P-gp. We confirmed that AT7159 (cyclin-dependent kinase inhibitor); AT9283, (Janus kinase 2/3 inhibitor); ispinesib (kinesin spindle protein inhibitor); gedatolisib (PKI-587, phosphoinositide 3-kinase/mammalian target of rampamycin inhibitor); GSK-690693 (AKT inhibitor); and KW-2478 (heat shock protein 90 inhibitor) were substrates, and direct ATPase stimulation was assessed. ABCG2 was also found to confer high levels of resistance to AT9283, GSK-690693 and gedatolisib, while ispinesib, AT7519 and KW-2478 were weaker substrates. Combinations of P-gp substrates and inhibitors were assessed to demonstrate on-target synergistic cell killing. These data identify compounds for which oral bioavailability or brain penetration may be affected by P-gp.

Molecular Pharmacology Fast Forward. Published on September 12, 2019 as DOI: 10.1124/mol.119.115964
This article has not been copyedited and formatted. The final version may differ from this version.

Significance statement

The ATP-binding cassette transporter P-glycoprotein (P-gp) is known to be expressed at barrier sites where it acts to limit oral bioavailability and brain penetration of substrates. In order to identify novel compounds that are transported by P-gp, we developed a high-throughput screen using the KB-3-1 cancer cell line and its colchicine selected subline, KB-8-5-11. We screened the Mechanism Interrogation Plate (MIPE) library, the NCATS pharmaceutical collection (NPC), the NCATS Pharmacologically Active Chemical Toolbox (NPACT), and a kinase inhibitor library comprised of 977 compounds, for a total of 10,804 compounds. Of the 10,804 compounds screened, a total of 90 substrates were identified of which 55 were novel. P-gp expression may adversely affect the oral bioavailability or brain penetration of these compounds.

Molecular Pharmacology Fast Forward. Published on September 12, 2019 as DOI: 10.1124/mol.119.115964
This article has not been copyedited and formatted. The final version may differ from this version.

Introduction

The ATP-binding cassette (ABC) transporters P-glycoprotein (P-gp, encoded by the *MDR1* gene and later renamed *ABCB1*) and ABCG2 (or breast cancer resistance protein, encoded by the *ABCG2* gene) play major roles in limiting the oral bioavailability of compounds and preventing drug ingress at the blood-brain barrier (BBB) by keeping toxins, drugs, and other compounds out of the brain (Gottesman et al., 2016). Soon after its identification as a drug transporter, P-gp was found to be expressed in the small intestine and colon, liver, pancreas, and kidney (Thiebaut et al., 1987), and pharmacokinetic studies in mice deficient for one of the murine homologs of human *ABCB1*, *Mdr1a* (renamed *Abcb1a*) demonstrated increased bioavailability of orally-administered taxol compared to wild-type mice (Sparreboom et al., 1997). Likewise, ABCG2 was detected in the small intestine and colon (Fetsch et al., 2006; Maliepaard et al., 2001) and the role of ABCG2 in limiting oral uptake of topotecan was confirmed in mice lacking *Abcg2*, the murine homolog of *ABCG2* (Basseville et al., 2016; Jonker et al., 2000).

In addition to being highly expressed in the gastrointestinal tract, in the brush border of renal proximal tubule cells and on the apical surface of hepatocytes (Fetsch et al., 2006; Huls et al., 2008; Thiebaut et al., 1987), both P-gp and ABCG2 are expressed at high levels on the apical side of capillary endothelial cells in the brain (Cooray et al., 2002; Cordon-Cardo et al., 1989; Thiebaut et al., 1987; Thiebaut et al., 1989). The protective role of P-gp was demonstrated in 1994 when Schinkel and colleagues found that deletion of *Abcb1a* in mice resulted in acute sensitivity to the acaricide ivermectin due to a 90-fold increase in brain penetration of the drug (Schinkel et al., 1994). Brain penetration of the P-gp substrate drug vinblastine was increased 20-fold in *Abcb1a*-deficient mice (Schinkel et al., 1994). Subsequent to the discovery of ABCG2,

Molecular Pharmacology Fast Forward. Published on September 12, 2019 as DOI: 10.1124/mol.119.115964
This article has not been copyedited and formatted. The final version may differ from this version.

mice deficient in the two murine homologs of human ABCB1 (*Abcb1a*/*1b*) and *Abcg2* were generated. The murine models highlighted a compensatory and possibly a cooperative role for the two transporters at the BBB limiting the brain penetration of chemotherapeutic agents, in particular kinase inhibitors (Basseville et al., 2016). In a recent example, 24 h after mice were given an oral dose of the BCR-ABL kinase inhibitor ponatinib, mice lacking *Abcg2* expression had a 2.2-fold increase in brain concentration compared to wild-type mice, while mice lacking *Abcb1a/1b* had a 1.9-fold increase and mice lacking *Abcb1a/1b* and *Abcg2* had a 25.5-fold increase (Kort et al., 2017). The mouse studies highlight not only the protective and complementary role of the transporters at the BBB but also their importance in thwarting effective delivery of chemotherapy to the brain (Robey et al., 2018). However, mouse models may slightly overestimate the contribution of P-gp at the human BBB, due to higher levels at the mouse BBB (Chu et al., 2013).

Because transporters affect drug efficacy and pharmacokinetics, it is important to know which compounds are substrates. This can affect decisions on how a drug is administered or whether or not the drug might be effective in the treatment of neurological diseases, and against drug-resistant tumor cells. This information is also valuable for designing pre-clinical efficacy studies in mice. Although the FDA offers guidelines for determining the interaction of investigational drugs with P-gp and ABCG2 (Lee et al., 2017), often these critical data are not published.

We implemented a systematic screen to identify cytotoxic substrates of P-gp. To do so, we developed high-throughput assays to examine differential cell killing between drug-naïve cancer cell lines and drug-selected, P-gp-overexpressing sublines. We screened several libraries of annotated compounds including the NCATS Pharmaceutical Collection (NPC), a

comprehensive collection of all clinically approved drugs, along with small molecules with known mechanisms of action – either as probe small molecules or experimental therapeutics designed to modulate a wide range of targets, including many small molecules developed for oncology indications. Mechanistic annotation of these compounds can provide valuable insight into targets or pathways that appear to have been rendered more sensitive to inhibition in the course of multidrug resistance development. Hits from the primary screen were assessed against HEK cells over-expressing P-gp in the absence and presence of the P-gp inhibitor tariquidar. Top substrates were tested in a cell-killing synergy experiment with the inhibitors tariquidar or elacridar, demonstrating the consistent inhibition of P-gp by inhibitors irrespective of substrate.

Materials and Methods

Cell Lines. The HeLa derivative cell line, KB-3-1, and its colchicine-selected, P-gp-overexpressing subline, KB-8-5-11 (Shen et al., 1986) were maintained in DMEM with 10% FCS and Pen/Strep with glutamine at 37°C in 5% CO_2. For KB-8-5-11 cells, colchicine was added to the medium at a concentration of 100 ng/mL. HEK-293 cells transfected with empty vector (pcDNA) or vector containing human *ABCB1* (MDR-19) or *ABCG2* (R-5) have been described previously (Robey et al., 2011) and were maintained in EMEM supplemented with 10% FCS, Pen/Strep and glutamine with 2 mg/ml G418 to select for the expression of the transporter. Cultures were confirmed to be free of mycoplasma infection using the MycoAlert Mycoplasma Detection Kit (Lonza, Walkersville, MD). For the screen, assay medium was identical to culture medium except for KB-8-5-11 where colchicine was excluded from the medium.

Molecular Pharmacology Fast Forward. Published on September 12, 2019 as DOI: 10.1124/mol.119.115964
This article has not been copyedited and formatted. The final version may differ from this version.

Screening Libraries. The libraries that were used for the screen included the Mechanism Interrogation Plate (MIPE) comprised of 1,912 compounds (Mathews Griner et al., 2014), the NCATS pharmaceutical collection (NPC) comprised of 2816 compounds (Huang et al., 2011), the NCATS Pharmacologically Active Chemical Toolbox (NPACT) (Davis et al., 2016) comprised of 5,099 compounds, and a kinase inhibitor library comprised of 977 compounds, for a total of 10,804 compounds.

High Throughput Screen (HTS). All cell lines were plated into 1536-well plates at 500 cells/well in 5 μL media. Compounds were then pinned in dose-response using a 1536-head pin tool (Kalypsis, San Diego, CA) and plates were incubated at 37 °C in 5% CO_2 for an additional 72 h. CellTiter-Glo reagent (Promega) was dispensed into the wells, incubated for 5 min and luminescence was read on a ViewLux instrument (Perkin-Elmer). To determine compound activity in the qHTS assay, the concentration-response data for each sample was plotted and modeled by a four parameter logistic fit yielding IC_{50} and efficacy (maximal response) values as previously described (Inglese et al., 2006). Usually the qHTS screen yielded hits with a wide range of potencies and with substantial variation in the quality of the corresponding concentration-response curves (CRCs) (efficacy and number of asymptotes), which included samples associated with shallow curves or single-point extrapolated concentration responses; these were assigned as low-confidence actives. In brief, Class -1.1 and -1.2 were the highest-confidence complete CRCs containing upper and lower asymptotes with efficacies ≥ 80% and < 80%, respectively. Class -2.1 and -2.2 were incomplete CRCs having only one asymptote with efficacy ≥ 80% and < 80%, respectively. Class -3 CRCs showed activity at only the highest concentration or were poorly fit. Class 4 CRCs were inactive, having a curve-fit of insufficient

Molecular Pharmacology Fast Forward. Published on September 12, 2019 as DOI: 10.1124/mol.119.115964
This article has not been copyedited and formatted. The final version may differ from this version.

efficacy or lacking a fit altogether. High confidence cytotoxic compounds were defined as those that yielded a curve class of -1.1, -1.2, -2.1, -2.2, a maximum response of $\geq$50% and an AC50 of $\leq$ 10μM.

Compounds were further clustered hierarchically using TIBCO Spotfire 6.0.0 (Spotfire Inc., Cambridge, MA. https://spotfire.tibco.com/) based on their activity outcomes from the primary or follow up screen across different cell lines. Area-under-the-curve (AUC) for each compound was calculated based on the qHTS data analysis and curve fittings were utilized for clustering. In the heatmap, darker color indicates compounds that are more potent and efficacious, i.e. high-quality actives, and lighter color indicates less potent and efficacious compounds. If a compound didn't show any activity in an assay, it was highlighted as white in the heatmap.

Cherry-picked hits from screening analysis were tested with both the KB pair of cell lines, and the pcDNA (empty vector control) and MDR-19 (P-gp overexpressing) pair were tested, in the absence and presence of tariquidar. Confirmatory three-day cytotoxicity assays were also performed by plating pcDNA, MDR-19 or R-5 cells in 96-well, opaque white plates at a density of 5,000 cells/well and allowing them to attach overnight. Compounds were added at increasing concentrations and incubated with the cells for 72 h after which plates were analyzed using CellTiter-Glo according to the manufacturer's instructions. GI_{50} (50% growth inhibitory concentration) values were obtained by determining the drug concentration for which the luminescence value was 50% of that obtained for untreated cells.

Synergy Experiments. Synergy screens were performed with a subset of P-gp substrates identified by HTS in combination with the P-gp inhibitors tariquidar or elacridar. Plating of

compounds in matrix format using acoustic droplet ejection and numerical characterization of synergy, additivity and/or antagonism were conducted as described previously (Martinez et al., 2016; Mathews Griner et al., 2014). Briefly, compounds were plated as a 10 x 10 dose response combination matrix. Concentration ranges were selected from single agent dose response curves generated from the HTS. Compounds were acoustically dispensed (10 nL/well) using an ATS-100 (EDC Biosystems) onto 1,536-well, white, solid-bottom, TC-treated plates. KB-3-1 and KB-8-5-11 cells were subsequently added to the plates (500 cells/well in 5 µl) and incubated for 72 hr at 37°C with 5% CO_2 under 85% humidity. Cell viability was determined by the addition of 2.5 µL of CellTiter-Glo into to each well. After 15 min incubation at RT, each sample's luminescence intensity was measured using a ViewLux reader. DMSO (20 nL) and bortezomib (20 nL at 2.3 mM) were used as negative and positive controls, respectively. All P-gp substrates listed in Table 1 were tested against the P-gp inhibitors tariquidar and elacridar. Viability resulting from a single agent or combination was normalized to a separate negative control column (20 nL DMSO). The synergies were characterized using the Bliss independence model and summarized using the DBSumNeg metric. In brief, the Bliss independence model expected no mechanistic interaction between two tested compounds. Therefore, the viability from an additive dose combination ($C_{additive}$) is the multiplication of factional viability upon treatment of compound X and Y individually, $C_{additive} = X \times Y$ ($0 \leq X \leq 1$, $0 \leq Y \leq 1$). The difference between measured viability and expected viability from an additive dose combination ($C_{measured} - C_{additive}$), so called deltaBliss (DB), describes the additivity ($DB = 0$), synergy ($DB < 0$) or antagonistism ($DB > 0$). To evaluate the overall synergy from all 81 dose combinations we tested in a 10 x 10 block, we calculated DBSumNeg as the sum of all negative DB.

Molecular Pharmacology Fast Forward. Published on September 12, 2019 as DOI: 10.1124/mol.119.115964
This article has not been copyedited and formatted. The final version may differ from this version.

ATPase Assay. The ATPase assay was performed as described previously (Ambudkar, 1998). Briefly, crude membrane protein (100 μg/ml) was isolated from Hi-Five insect cells expressing human P-gp. The vanadate-sensitive activity was calculated by measuring the end point phosphate release assay in the absence and presence of vanadate. Briefly, solutions containing 4.0 μg of total membrane protein in 100 μL of ATPase assay buffer (50 mM MES-Tris pH 6.8, 50 mM KCl, 5 mM sodium azide, 1 mM EGTA, 1 mM ouabain, 2 mM DTT, 10 mM $MgCl_2$) with 1% DMSO solvent alone (basal activity) or with variable concentrations (0.1, 1 or 10 μM) of the substrates in DMSO were prepared. The tubes were incubated for 3 min at 37°C, after which the reaction was initiated by addition of 5 mM ATP. After 20 min, the reaction was stopped by the addition of 2.5% SDS. The amount of inorganic phosphate released was quantified by a colorimetric method, as previously described (Ambudkar, 1998). Significance between various treatments was determined by a one-way ANOVA followed by a Dunnet test for multiple comparisons. A p value of less than 0.05 was considered significant.

Flow Cytometry. Transport assays were conducted as described previously (Robey et al., 2004). To measure inhibition of P-gp-mediated transport, trypsinized MDR-19 cells were incubated in phenol red-free IMEM supplemented with 10% FCS, Pen/Strep, and glutamine, containing 0.5 μg/mL rhodamine 123 (Sigma-Aldrich, St. Louis MO) in the presence or absence of 25 μM of selected compounds identified by the screen for 30 min at 37°C in 5% CO_2. The medium was then removed and replaced with complete medium with or without the compound for an additional 1 h. Valspodar (Apex Biotechnology, Houston, TX) at 3 μg/mL served as a positive control for P-gp inhibition. For ABCG2-mediated transport, R-5 cells were incubated in a similar fashion except 5 μM pheophorbide A (PhA, Frontier Scientific, Logan, UT) was used

as the substrate and 10 μM fumitremorgin C (FTC, synthesized by the NIH Chemical Biology Laboratory, Bethesda, MD) served as the positive control for ABCG2 inhibition. Samples were analyzed on a FACSCanto II flow cytometer (BD Biosciences, San Jose, CA) in which rhodamine fluorescence was detected with a 488-nm argon laser and a 530-nm bandpass filter and PhA was detected using a 635-nm red diode laser and a 670-nm filter. At least 10,000 events were collected for each sample.

Results

High-throughput Screen to Identify P-gp Substrates. To identify novel substrates of P-gp, we used the CellTiter-Glo luminescent cell viability assay to test library compounds against three cell conditions: (1) the parental KB-3-1 human cervical adenocarcinoma cell line (a HeLa clone); (2) the drug-resistant subline KB-8-5-11 that over-expresses P-glycoprotein, and (3) the KB-8-5-11 cell line in the presence of the P-gp inhibitor tariquidar (which should restore sensitivity to P-gp substrates). Overall, 10,804 compounds were tested from across four annotated small molecule libraries. The NCATS Pharmaceutical Collection (NPC) is a library of compounds approved for use by the Food and Drug Administration and related agencies in foreign countries. The NCATS Pharmacologically Active Chemical Toolbox (NPACT) library contains pre-clinical and probe compounds from across disease areas. The kinase inhibitor library contains almost 1,000 small molecule inhibitors of kinases, with known mechanisms of action. The Mechanism Interrogation PlatE (MIPE) library contains oncology-focused compounds with known mechanisms of action.

Molecular Pharmacology Fast Forward. Published on September 12, 2019 as DOI: 10.1124/mol.119.115964
This article has not been copyedited and formatted. The final version may differ from this version.

The screen was designed based on the fundamental principle of P-gp-mediated drug resistance: substrates which kill or inhibit growth of KB-3-1 were expected to demonstrate reduced efficacy against the KB-8-5-11 cells due to drug efflux by P-gp. P-gp-specific efflux could be demonstrated by sensitization of KB-8-5-11 cells in the presence of the P-gp inhibitor tariquidar. As a cell viability assay was utilized for this screen, a limitation of the screen is that only cytotoxic or cytostatic P-gp substrates could be identified. Of 10,804 compounds tested, 1,362 compounds demonstrated cytotoxicity towards the KB-3-1 cells, of which 90 compounds were identified as putative P-gp substrates (Fig. 1A). In total, 13% of all compounds tested demonstrated cytotoxicity towards the parental KB-3-1 cell line. Among the four libraries, the kinase inhibitor library (30%) and oncology-focused MIPE library (21%) contained the greatest proportion of cytotoxic compounds, followed by the NPACT library (10%) (Fig. 1B). As one might anticipate, the NPC library of therapeutic agents contained the lowest proportion of cytotoxic compounds (5%).

A comparison of the global response of the two cell lines to the library compounds was undertaken by assessing the area-under-the-curve for each compound against each cell line (Fig. 1C). The AUC of the dose-response curve ensures both efficacy (magnitude of cell killing) and potency (concentration that elicits cell killing) are accounted for in the analysis of activity (Fig. 1A). The KB-3-1 cell line was more sensitive than the KB-8-5-11 cell line for a number of compounds, shown in Fig. 1C, where darker red correlates with greater sensitivity to a given compound (the compound is more cytotoxic), while lighter colors correlate with more resistance. This is consistent with the multidrug-resistant nature of the KB-8-5-11 cell line.

To pinpoint substrates identified by HTS, the difference in AUC between KB-3-1 and KB-8-5-11 cells was determined. As an example, the HTS dose-response curves for vincristine

Molecular Pharmacology Fast Forward. Published on September 12, 2019 as DOI: 10.1124/mol.119.115964
This article has not been copyedited and formatted. The final version may differ from this version.

(a known P-gp substrate) are displayed in Fig. 2A for all three conditions screened. As cell killing assays involve loss of signal, data were analyzed from 0% (positive control signal) to -100% (complete cell killing/growth inhibition). The data represented in Fig. 2A is usual for HTS data analysis, but not normal for displaying cell killing data – elsewhere in this manuscript, data are displayed as is traditional for cell killing assays with 100% as control cell viability and 0% as total cell death. The difference (delta) between the AUC for the sensitive KB-3-1 cell line (black line) and the resistant KB-8-5-11 cell line (red line) was determined (termed ΔAUC1, Fig. 2A), and the greater the magnitude of ΔAUC1, the stronger the substrate effect of P-gp. This strategy is distinct from the commonly applied method used to discern P-gp substrates by comparing the IC_{50} values derived from dose-response curves. The difference between KB-8-5-11 cells with (blue line) and without (red line) the P-gp inhibitor tariquidar (1 μM) was also assessed in order to confirm P-gp substrates (termed ΔAUC2). The P-gp primary high-throughput screening data for KB-3-1 and KB-8-5-11 cell lines against NPC, NPACT MIPE and Kinase libraries was deposited in PubChem with AIDs 1346986 and 1346987, respectively. Assay data can be accessed via the following links: https://pubchem.ncbi.nlm.nih.gov/assay/assay.cgi?aid=1346986 for the KB-3-1 cell line, and https://pubchem.ncbi.nlm.nih.gov/assay/assay.cgi?aid=1346987 for the KB-8-5-11 cell line.

Following plating of hits and re-testing for confirmation, a total of 90 P-gp substrates were identified (Supplementary Table 1) based on a ΔAUC1 cut-off value of 50. Comparison of identified substrates with the literature revealed 35 known P-gp substrates were identified in the screen, and 55 new substrates were identified. Comparison of ΔAUC1 and ΔAUC2 for all substrates revealed a strong correlation between parental cells and inhibited KB-8-5-11 cells in

Molecular Pharmacology Fast Forward. Published on September 12, 2019 as DOI: 10.1124/mol.119.115964
This article has not been copyedited and formatted. The final version may differ from this version.

which P-gp was inhibited with tariquidar (Fig. 2B). To confirm that the putative P-gp substrates were not due to cell line-specific alterations, an orthogonal assay testing all hits against HEK 293 human embryonic kidney cells stably transfected with either plasmid control (pcDNA) or a plasmid expressing *ABCB1* (MDR-19), was conducted and and ΔAUC1 was calculated. A correlation was demonstrated between the KB-3-1/KB-8-5-11 ΔAUC1 and the pcDNA/MDR-19 ΔAUC1 (Fig. 2C). Unsupervised clustering of global cell response to the 90 substrates identified for the three KB and three HEK conditions (parent, resistant, resistant with tariquidar) demonstrated a consistent pattern, with the KB-8-5-11 and MDR-19 cell lines less sensitive to compounds compared to their parental partners, and the parent lines clustering with the resistant cell lines in the presence of tariquidar (Fig. 2D).

Assessment of P-gp Substrates. To confirm that the HTS assay and analysis strategy identifies substrates, we assessed the cell-killing activity of three known substrates included in the library (target in brackets): paclitaxel [tubulin] (Greenberger et al., 1988), vincristine [tubulin] (Horton et al., 1987), and mithramycin [RNA synthesis] (Biedler and Riehm, 1970) (Fig. 3A-C, respectively). Examples of the dose-response curves for three newly identified substrates are PKI-402 [PI3K/mTOR](Dehnhardt et al., 2010), CB300919 [NAMPT](Bavetsias et al., 2002), and PHA-793887 [CDK1/2/4](Brasca et al., 2010) (Fig. 3D-F, respectively). In each case, a strong difference in cell killing between parent and resistant cells was found.

To confirm that the newly identified substrates were indeed P-gp substrates, we performed confirmatory cytotoxicity assays in the laboratory using pcDNA and MDR-19 cells. We selected 6 commercially available, newly-identified P-gp substrates AT7159, a cyclin-dependent kinase (CDK) inhibitor; AT9283, a JAK2/3 inhibitor; ispinesib, a kinesin spindle

protein inhibitor; gedatolisib (PKI-587), a PI3K/mTOR inhibitor; GSK-690693, an AKT inhibitor; and KW-2478, an HSP90 inhibitor. In addition, we examined the ability of ABCG2 to confer resistance to the compounds using ABCG2-overexpressing R-5 cells. As shown in Table 1, all of the compounds were confirmed to be P-gp substrates, with P-gp expression conferring less resistance to AT9283 (13-fold), but conferring very high levels of resistance to gedatolisib (1672-fold). All of the compounds were also found to be ABCG2 substrates to varying degrees. In the case of AT9283, GSK-690693 and gedatolisib, ABCG2 conferred relatively high levels of resistance, while ispinesib, AT7519 and KW-2478 were preferentially transported by P-gp.

Effect of Newly-Identified Substrates on ATPase Activity of P-gp. The ability of substrates to stimulate the ATPase activity of P-gp was assessed. Some kinase inhibitors that are P-gp substrates have been shown to significantly stimulate the ATPase activity of P-gp, while others do not (Hegedus et al., 2009). The ATPase assay is regularly used to confirm the binding of a substrate to the protein; inhibitors tend to decrease the ATPase activity, transport substrates generally enhance the ATPase activity. However, not all substrates increase ATPase activity. We omitted AT9283 from this assay, as P-gp conferred the lowest levels of resistance to this compound. The vanadate-sensitive ATPase activity of P-gp in the presence of 0.1, 1 or 10 μM of each compound compared with the basal activity (activity in the presence of 1% DMSO). As observed in Fig. 4A-E, we found that ispinesib stimulated ATPase activity in a concentration-dependent manner. Ispinesib stimulated the ATPase activity by >2.6 fold at concentrations greater than 1 μM (1.6 fold at 0.1 μM). KW-2478 was also capable of stimulating the ATPase activity, but only at higher concentrations (10 μM) and only up to 1.4-fold. The rest of the compounds did not significantly affect the ATPase activity in the range of concentrations tested.

Molecular Pharmacology Fast Forward. Published on September 12, 2019 as DOI: 10.1124/mol.119.115964
This article has not been copyedited and formatted. The final version may differ from this version.

As a positive control, verapamil at 10 μM is shown to increase the ATPase activity of P-gp by approximately 2.5-fold (Fig. 4F).

P-gp Inhibitors Synergize With Substrates. P-gp substrates were identified during the HTS in part by co-treating P-gp-expressing cells with the inhibitor tariquidar at a concentration (1 μM) shown to fully inhibit P-gp, to demonstrate P-gp-specific resistance. To explore the nature of inhibitor-mediated sensitization of substrates, we assessed 10 x 10 combinations of tariquidar or elacridar with 15 P-gp substrates identified from the screen (Table 2). Viability was again measured using CellTiter-Glo, and the Bliss independence model was used to characterize the presence or absence of synergy for each combination, where negative ΔBliss represents synergy, and positive ΔBliss represents antagonism. We hypothesized that inhibitors should antagonize P-gp transport of substrates in P-gp-expressing cells, and that this approach could be used to compare the efficacy of P-gp inhibitors in combination with a range of substrates. This approach has not been previously adopted for studying ABC transporter inhibitors.

The effect of both tariquidar and elacridar across all substrates was uniform. Paclitaxel is shown as an example. Parental KB-3-1 cells were sensitive to paclitaxel (black = 100% viable, red = 0% viable), and this sensitivity was unaffected by addition of elacridar up to a concentration of 20 μM (Fig. 5A). This is exemplified by the absence of any strong synergy (red) or antagonism (blue) (Fig. 5A), and in paclitaxel dose-response curves extracted from the 10 x 10 block (Fig. 5B). This relationship was observed for both inhibitors in combination with every P-gp substrate tested against parental cells. Elacridar and tariquidar alone had no effect on cell viability. The 10 x 10 blocks for parental KB-3-1 cell are available at https://tripod.nih.gov/matrix-client/rest/matrix/blocks/8067/table.

Molecular Pharmacology Fast Forward. Published on September 12, 2019 as DOI: 10.1124/mol.119.115964
This article has not been copyedited and formatted. The final version may differ from this version.

In contrast, the P-gp substrates demonstrated maximal synergy in combination with elacridar and tariquidar in P-gp-expressing KB-8-5-11 cells. The combination of paclitaxel and elacridar is shown as an example (Fig. 5C, D). In the absence of elacridar, paclitaxel demonstrated minimal cytotoxicity towards KB-8-5-11 cells, but addition of elacridar sensitized the cells to paclitaxel, with near-maximal effects at 82 nM and higher. Dose-response curves from the 10 x 10 block demonstrate the sensitization of KB-8-5-11 cells to paclitaxel with increasing elacridar concentration (Fig. 5C), and this sensitization was accompanied by maximal synergy. Synergy was observed for both inhibitors in combination with every P-gp substrate tested against P-gp-expressing KB-8-5-11 cells. The 10 x 10 blocks for P-gp-expressing KB-8-5-11 cell are available at https://tripod.nih.gov/matrix-client/rest/matrix/blocks/8069/table.

To ascertain the inhibitory potency of tariquidar and elacridar, dose-response curves were extracted from the 10 x 10 block of each inhibitor against each compound. 13 of 15 compounds elicited near-complete cell killing, the exceptions being the Aurora kinase inhibitors tozasertib and danusertib, which had a maximal efficacy of approximately 50% (Fig. 5E, F). Tariquidar (Fig. 5E) and elacridar (Fig. 5F) both achieved near-complete inhibition of all compounds (maximal cell killing) at 247 nM, and the average IC_{50} against fifteen diverse substrates were 100 ± 49 nM (cotreated with tariquidar) and 84 ± 48 nM (cotreated with elacridar), suggesting inhibition of P-gp irrespective of the substrate. IC_{50}s for inhibition of compounds were consistent with values in the literature, though there are no studies comparing inhibitors and testing them against a large number of substrates.

Newly-Identified P-gp Substrates Inhibit P-gp- and ABCG2-Mediated Transport. Many P-gp substrates have also been found to inhibit P-gp-mediated transport at relatively high

concentrations and this is particularly true for kinase inhibitors (Durmus et al., 2015). We next assessed the ability of the six compounds tested earlier (see Table 1) to inhibit P-gp-mediated rhodamine 123 transport or ABCG2-mediated pheophorbide A transport from MDR-19 or R5 cells, respectively, as shown in Fig. 6. At a concentration of 25 μM, only ispinesib was found to appreciably inhibit P-gp-mediated rhodamine transport and was nearly as effective as 3 μM valspodar (Fig. 6A). Ispinesib was also the only compound found to appreciably inhibit pheophorbide A transport, although not as well as fumitremorgin C, which served as a positive control for ABCG2 inhibition (Fig. 6B). In agreement with previous reports, we find that some kinase inhibitors are substrates of transporters at low concentrations, but then act as inhibitors at higher concentrations.

Discussion

P-gp and ABCG2 are known to play a role in the disposition of many toxins by limiting oral bioavailability, increasing excretion, and limiting brain penetration (Robey et al., 2018). While many targeted therapies have been developed, often it is unclear what role transporters might play in their disposition and how they might affect therapy. We therefore developed a high-throughput screening assay to identify novel substrates of P-gp. Using KB-3-1 cells that do not express P-gp and their P-gp-overexpressing KB-8-5-11 counterpart, we identified 55 novel substrates of P-gp that were confirmed in a second pair of cell lines both in the primary screen and secondary assays. These data may have value in identifying compounds for which drug-drug interactions might be a concern. Alternatively, knowing whether a compound is a P-gp substrate may be helpful for determining the best route of administration in pre-clinical, mouse model studies. Additionally, this information may be valuable to researchers who are testing novel

treatments or combinations for brain cancers or metastases in mice, as compounds that are transported by P-gp will most likely not cross the blood-brain barrier, as shown by mouse knockout models (Robey et al., 2018).

Previous screens have used alternative methods to identify novel P-gp substrates. The NCI-60 drug screen cell line set was previously used to identify P-gp substrates based on measuring rhodamine 123 transport (Lee et al., 1994) or *ABCB1* gene expression data (Alvarez et al., 1995; Szakacs et al., 2004) in the 60 cell lines of the screen and comparing that to drug sensitivity profiles. Cell lines with higher levels of P-gp expression were found to correlate with decreased sensitivity to substrate drugs. This method was successful due to the relatively high level of variation of P-gp expression in the lines of the screen. In the case of ABCC1 or ABCG2, with cells expressing much lower levels of the transporters, the screen was less successful and often did not identify known substrates (Alvarez et al., 1998; Deeken et al., 2009). More recently our group developed an assay based on a dual-fluorescent system, in which sensitive cells (OVCAR8) were transduced to express DsRed red fluorescent protein and P-gp overexpressing cells (NCI/ADR-RES) expressed enhanced green fluorescent protein (Brimacombe et al., 2009).

The present study, and those referenced above, rely on P-gp to protect cells from cell death. While appropriate for a study such as this examining cancer drug resistance, a limitation of this approach is that non-toxic compounds cannot be studied. Strategies for studying non-toxic substrates have been explored, and rely on either direct monitoring of the test compounds (for example, radioactivity or analytical detection), or interference with the efflux of a fluorescent substrate. The primary example of the latter comes from Sklar and co-workers, who have reported a number of screens using flow cytometry to identify inhibitors of ABC transporters

(Ivnitski-Steele et al., 2008; Strouse et al., 2013a; Strouse et al., 2013b; Winter et al., 2008). A Pfizer study reported a correlation between MDCK cells transfected with mouse (Mdr1a) and human (MDR1) P-gp for 3300 compounds, using LC-MS for analytical quantitation of each compound, although the compounds themselves were not disclosed (Feng et al., 2008). Further work is needed to tabulate all pharmacologically active drugs that are P-gp substrates.

Of course, high-throughput screening methods do have limitations. First, the compounds must be toxic and/or cause cell cycle arrest so that differences between treated and untreated cells can be detected by the CellTiter Glo assay. Thus, the assay will not detect all substrates. Additionally, the ability of a drug to inhibit growth or elicit toxicity often depends on the choice of cell line model. For example, while mutant BRAF inhibitors were among the compounds tested, none emerged as potential substrates despite the fact that some of them such as vemurafenib and dabrafenib were reported to be substrates of P-gp (Mittapalli et al., 2013; Mittapalli et al., 2012). This is not unexpected, as the cell line model systems we used did not harbor a mutant BRAF gene. Among the substrates identified, there were no MEK inhibitors, although trametinib and cobimetinib are both known to be P-gp substrates (Choo et al., 2014; de Gooijer et al., 2017). This is most likely due to the fact that the cell line models used did not harbor mutations in BRAF or Ras. Therefore, while this assay did identify several new substrates of P-gp, it does not represent a definitive way to determine if a compound is a P-gp substrate.

Synergy is an important concept in combination chemotherapy, but it is not often discussed in the context of transport inhibitors. Utilizing the Bliss calculation, we demonstrated the profound synergy that inhibition of P-gp can produce in combination with avid P-gp substrates. An advantage of the 10 x 10 combination grid is the ability to readily examine the effects of inhibitors on P-gp substrates. After the initial screen, the ability of the inhibitors

Molecular Pharmacology Fast Forward. Published on September 12, 2019 as DOI: 10.1124/mol.119.115964
This article has not been copyedited and formatted. The final version may differ from this version.

tariquidar and elacridar were tested in increasing concentrations with the 17 substrates identified by the screen. Both inhibitors were found to synergize with the substrates, and to act at a consistent concentration in combination with all compounds tested. The sensitivity of the synergy screening approach suggests that it may be an alternative strategy to identify P-gp substrates, and could potentially be used to detect non-cytotoxic substrates that are also competitive inhibitors.

In conclusion, we developed a high-throughput screen to identify substrates of P-gp. We identified 55 novel substrates, among them targeted therapies that have yet to be developed clinically. We also have demonstrated that our method can be easily used to confirm the action of proposed P-gp inhibitors by sensitizing P-gp-overexpressing cells to numerous substrates. Future studies will focus on translating these techniques to the identification of substrates of other ABC transporters.

Acknowledgements

We appreciate the technical assistance of George Leiman. The content of this publication does not necessarily reflect the views or policies of the Department of Health and Human Services, nor does mention of trade names, commercial products, or organizations imply endorsement by the U.S. Government.

Authorship Contributions

Participated in research design: TDL, OWL, KRB, CKT, RWR, SVA, MMG, MDH

Conducted experiments: TDL, OWL, LC, RG, SL, BGT, RWR

Performed data analysis: TDL, OWL, LC, RG, SL, RWR, SVA, MS

Wrote or contributed to the writing of the manuscript: TDL, SL, RWR, MDH

References

Alvarez M, Paull K, Monks A, Hose C, Lee JS, Weinstein J, Grever MR, Bates SE and Fojo AT (1995) Generation of a drug resistance profile by quantitation of mdr-1/P-glycoprotein in the cell lines of the NCI anticancer drug screen. *JClinInvest* **95**: 2205-2214.

Alvarez M, Robey R, Sandor V, Nishiyama K, Matsumoto Y, Paull K, Bates S and Fojo T (1998) Using the national cancer institute anticancer drug screen to assess the effect of MRP expression on drug sensitivity profiles. *Mol Pharmacol* **54**: 802-814.

Ambudkar SV (1998) Drug-stimulatable ATPase activity in crude membranes of human MDR1-transfected mammalian cells. *Methods Enzymol* **292**: 504-514.

Basseville A, Hall MD, Chau CH, Robey RW, Gottesman M, Figg WD and Bates SE (2016) The ABCG2 Multidrug Transporter, in *ABC Transporters - 40 Years on* (George MA ed) pp 195-226, Springer International Publishing, Cham.

Bavetsias V, Skelton LA, Yafai F, Mitchell F, Wilson SC, Allan B and Jackman AL (2002) The design and synthesis of water-soluble analogues of CB30865, a quinazolin-4-one-based antitumor agent. *J Med Chem* **45**: 3692-3702.

Biedler JL and Riehm H (1970) Cellular resistance to actinomycin D in Chinese hamster cells in vitro: cross-resistance, radioautographic, and cytogenetic studies. *Cancer Res* **30**: 1174-1184.

Brasca MG, Albanese C, Alzani R, Amici R, Avanzi N, Ballinari D, Bischoff J, Borghi D, Casale E, Croci V, Fiorentini F, Isacchi A, Mercurio C, Nesi M, Orsini P, Pastori W, Pesenti E, Pevarello P, Roussel P, Varasi M, Volpi D, Vulpetti A and Ciomei M (2010) Optimization of 6,6-dimethyl pyrrolo[3,4-c]pyrazoles: Identification of PHA-793887, a potent CDK inhibitor suitable for intravenous dosing. *Bioorg Med Chem* **18**: 1844-1853.

Brimacombe KR, Hall MD, Auld DS, Inglese J, Austin CP, Gottesman MM and Fung KL (2009) A dual-fluorescence high-throughput cell line system for probing multidrug resistance. *Assay Drug Dev Technol* **7**: 233-249.

Choo EF, Ly J, Chan J, Shahidi-Latham SK, Messick K, Plise E, Quiason CM and Yang L (2014) Role of P-glycoprotein on the brain penetration and brain pharmacodynamic activity of the MEK inhibitor cobimetinib. *Mol Pharm* **11**: 4199-4207.

Chu X, Bleasby K and Evers R (2013) Species differences in drug transporters and implications for translating preclinical findings to humans. *Expert Opin Drug Metab Toxicol* **9**: 237-252.

Cooray HC, Blackmore CG, Maskell L and Barrand MA (2002) Localisation of breast cancer resistance protein in microvessel endothelium of human brain. *Neuroreport* **13**: 2059-2063.

Cordon-Cardo C, O'Brien JP, Casals D, Rittman-Grauer L, Biedler JL, Melamed MR and Bertino JR (1989) Multidrug-resistance gene (P-glycoprotein) is expressed by endothelial cells at blood-brain barrier sites. *Proc Natl Acad Sci USA* **86**: 695-698.

Davis MI, Patrick SL, Blanding WM, Dwivedi V, Suryadi J, Golden JE, Coussens NP, Lee OW, Shen M, Boxer MB, Hall MD, Sharlow ER, Drew ME and Morris JC (2016) Identification of Novel Plasmodium falciparum Hexokinase Inhibitors with Antiparasitic Activity. *Antimicrob Agents Chemother* **60**: 6023-6033.

de Gooijer MC, Zhang P, Weijer R, Buil LCM, Beijnen JH and van Tellingen O (2017) The impact of P-glycoprotein and breast cancer resistance protein on the brain

pharmacokinetics and pharmacodynamics of a panel of MEK inhibitors. *Int J Cancer* **142**: 381-391.

Deeken J, Robey R, Shukla S, Steadman K, Chakraborty A, Poonkuzhali B, Schuetz E, Holbeck S, Ambudkar S and Bates S (2009) Identification of compounds that correlate with ABCG2 transporter function in the National Cancer Institute Anticancer Drug Screen. *Mol Pharmacol* **76**: 946-956.

Dehnhardt CM, Venkatesan AM, Delos Santos E, Chen Z, Santos O, Ayral-Kaloustian S, Brooijmans N, Mallon R, Hollander I, Feldberg L, Lucas J, Chaudhary I, Yu K, Gibbons J, Abraham R and Mansour TS (2010) Lead optimization of N-3-substituted 7-morpholinotriazolopyrimidines as dual phosphoinositide 3-kinase/mammalian target of rapamycin inhibitors: discovery of PKI-402. *J Med Chem* **53**: 798-810.

Durmus S, Hendrikx JJ and Schinkel AH (2015) Apical ABC transporters and cancer chemotherapeutic drug disposition. *Adv Cancer Res* **125**: 1-41.

Feng B, Mills JB, Davidson RE, Mireles RJ, Janiszewski JS, Troutman MD and de Morais SM (2008) In vitro P-glycoprotein assays to predict the in vivo interactions of P-glycoprotein with drugs in the central nervous system. *Drug Metab Dispos* **36**: 268-275.

Fetsch P, Abati A, Litman T, Morisaki K, Honjo Y, Mittal K and Bates S (2006) Localization of the ABCG2 mitoxantrone resistance-associated protein in normal tissues. *Cancer Lett* **235**(1): 84-92.

Gottesman MM, Lavi O, Hall MD and Gillet JP (2016) Toward a Better Understanding of the Complexity of Cancer Drug Resistance. *Annu Rev Pharmacol Toxicol* **56**: 85-102.

Greenberger LM, Lothstein L, Williams SS and Horwitz SB (1988) Distinct P-glycoprotein are overproduced in independently isolated drug-resistant cell lines. *ProcNatlAcadSciUSA* **85**: 3762-3766.

Hegedus C, Ozvegy-Laczka C, Apáti A, Magócsi M, Német K, Orfi L, Kéri G, Katona M, Takáts Z, Váradi A, Szakács G and Sarkadi B (2009) Interaction of nilotinib, dasatinib and bosutinib with ABCB1 and ABCG2: implications for altered anti-cancer effects and pharmacological properties. *Br J Pharmacol* **158**: 1153-1164.

Horton JK, Houghton PJ and Houghton JA (1987) Reciprocal cross-resistance in human rhabdomyosarcomas selected in vivo for primary resistance to vincristine and L-phenylalanine mustard. *Cancer Res* **47**: 6288-6293.

Huang R, Southall N, Wang Y, Yasgar A, Shinn P, Jadhav A, Nguyen DT and Austin CP (2011) The NCGC pharmaceutical collection: a comprehensive resource of clinically approved drugs enabling repurposing and chemical genomics. *Sci Transl Med* **3**: 80ps16.

Huls M, Brown CD, Windass AS, Sayer R, van den Heuvel JJ, Heemskerk S, Russel FG and Masereeuw R (2008) The breast cancer resistance protein transporter ABCG2 is expressed in the human kidney proximal tubule apical membrane. *Kidney Int* **73**: 220-225.

Inglese J, Auld DS, Jadhav A, Johnson RL, Simeonov A, Yasgar A, Zheng W and Austin CP (2006) Quantitative high-throughput screening: a titration-based approach that efficiently identifies biological activities in large chemical libraries. *Proc Natl Acad Sci U S A* **103**: 11473-11478.

Ivnitski-Steele I, Larson RS, Lovato DM, Khawaja HM, Winter SS, Oprea TI, Sklar LA and Edwards BS (2008) High-throughput flow cytometry to detect selective inhibitors of ABCB1, ABCC1, and ABCG2 transporters. *Assay Drug Dev Technol* **6**: 263-276.

Jonker JW, Smit JW, Brinkhuis RF, Maliepaard M, Beijnen JH, Schellens JH and Schinkel AH (2000) Role of breast cancer resistance protein in the bioavailability and fetal penetration of topotecan. *J Natl Cancer Inst* **92**: 1651-1656.

Kort A, van Hoppe S, Sparidans RW, Wagenaar E, Beijnen JH and Schinkel AH (2017) Brain Accumulation of Ponatinib and Its Active Metabolite, N-Desmethyl Ponatinib, Is Limited by P-Glycoprotein (P-GP/ABCB1) and Breast Cancer Resistance Protein (BCRP/ABCG2). *Mol Pharm* **14**: 3258-3268.

Lee JS, Paull K, Alvarez M, Hose C, Monks A, Grever M, Fojo AT and Bates SE (1994) Rhodamine efflux patterns predict P-glycoprotein substrates in the National Cancer Institute Drug Screen. *Mol Pharmacol* **46**: 627-638.

Lee SC, Arya V, Yang X, Volpe DA and Zhang L (2017) Evaluation of transporters in drug development: Current status and contemporary issues. *Adv Drug Deliv Rev* **116**: 100-118.

Maliepaard M, Scheffer GL, Faneyte IF, van Gastelen MA, Pijnenborg AC, Schinkel AH, van De Vijver MJ, Scheper RJ and Schellens JH (2001) Subcellular localization and distribution of the breast cancer resistance protein transporter in normal human tissues. *Cancer Res* **61**: 3458-3464.

Martinez NJ, Rai G, Yasgar A, Lea WA, Sun H, Wang Y, Luci DK, Yang SM, Nishihara K, Takeda S, Sagor M, Earnshaw I, Okada T, Mori K, Wilson K, Riggins GJ, Xia M, Grimaldi M, Jadhav A, Maloney DJ and Simeonov A (2016) A High-Throughput Screen Identifies 2,9-Diazaspiro[5.5]Undecanes as Inducers of the Endoplasmic Reticulum Stress Response with Cytotoxic Activity in 3D Glioma Cell Models. *PLoS One* **11**: e0161486.

Mathews Griner LA, Guha R, Shinn P, Young RM, Keller JM, Liu D, Goldlust IS, Yasgar A, McKnight C, Boxer MB, Duveau DY, Jiang JK, Michael S, Mierzwa T, Huang W, Walsh MJ, Mott BT, Patel P, Leister W, Maloney DJ, Leclair CA, Rai G, Jadhav A, Peyser BD, Austin CP, Martin SE, Simeonov A, Ferrer M, Staudt LM and Thomas CJ (2014) High-throughput combinatorial screening identifies drugs that cooperate with ibrutinib to kill activated B-cell-like diffuse large B-cell lymphoma cells. *Proc Natl Acad Sci U S A* **111**: 2349-2354.

Mittapalli RK, Vaidhyanathan S, Dudek AZ and Elmquist WF (2013) Mechanisms limiting distribution of the threonine-protein kinase B-RaF(V600E) inhibitor dabrafenib to the brain: implications for the treatment of melanoma brain metastases. *J Pharmacol Exp Ther* **344**: 655-664.

Mittapalli RK, Vaidhyanathan S, Sane R and Elmquist WF (2012) Impact of P-glycoprotein (ABCB1) and breast cancer resistance protein (ABCG2) on the brain distribution of a novel BRAF inhibitor: vemurafenib (PLX4032). *J Pharmacol Exp Ther* **342**: 33-40.

Robey RW, Lin B, Qiu J, Chan LL and Bates SE (2011) Rapid detection of ABC transporter interaction: potential utility in pharmacology. *J Pharmacol Toxicol Methods* **63**: 217-222.

Robey RW, Pluchino KM, Hall MD, Fojo AT, Bates SE and Gottesman MM (2018) Revisiting the role of ABC transporters in multidrug-resistant cancer. *Nat Rev Cancer* **18**: 452-464.

Robey RW, Steadman K, Polgar O, Morisaki K, Blayney M, Mistry P and Bates SE (2004) Pheophorbide a is a specific probe for ABCG2 function and inhibition. *Cancer Res* **64**: 1242-1246.

Schinkel AH, Smit JJ, van Tellingen O, Beijnen JH, Wagenaar E, van Deemter L, Mol CA, van der Valk MA, Robanus-Maandag EC and te Riele HP (1994) Disruption of the mouse

mdr1a P-glycoprotein gene leads to a deficiency in the blood-brain barrier and to increased sensitivity to drugs. *Cell* **77**: 491-502.

Shen DW, Fojo A, Chin JE, Roninson IB, Richert N, Pastan I and Gottesman MM (1986) Human multidrug-resistant cell lines: increased mdr1 expression can precede gene amplification. *Science* **232**: 643-645.

Sparreboom A, van Asperen J, Mayer U, Schinkel AH, Smit JW, Meijer DK, Borst P, Nooijen WJ, Beijnen JH and van Tellingen O (1997) Limited oral bioavailability and active epithelial excretion of paclitaxel (Taxol) caused by P-glycoprotein in the intestine. *Proc Natl Acad Sci U S A* **94**: 2031-2035.

Strouse JJ, Ivnitski-Steele I, Khawaja HM, Perez D, Ricci J, Yao T, Weiner WS, Schroeder CE, Simpson DS, Maki BE, Li K, Golden JE, Foutz TD, Waller A, Evangelisti AM, Young SM, Chavez SE, Garcia MJ, Ursu O, Bologa CG, Carter MB, Salas VM, Gouveia K, Tegos GP, Oprea TI, Edwards BS, Aubé J, Larson RS and Sklar LA (2013a) A selective ATP-binding cassette subfamily G member 2 efflux inhibitor revealed via high-throughput flow cytometry. *J Biomol Screen* **18**: 26-38.

Strouse JJ, Ivnitski-Steele I, Waller A, Young SM, Perez D, Evangelisti AM, Ursu O, Bologa CG, Carter MB, Salas VM, Tegos G, Larson RS, Oprea TI, Edwards BS and Sklar LA (2013b) Fluorescent substrates for flow cytometric evaluation of efflux inhibition in ABCB1, ABCC1, and ABCG2 transporters. *Anal Biochem* **437**: 77-87.

Szakacs G, Annereau JP, Lababidi S, Shankavaram U, Arciello A, Bussey KJ, Reinhold W, Guo Y, Kruh GD, Reimers M, Weinstein JN and Gottesman MM (2004) Predicting drug sensitivity and resistance: profiling ABC transporter genes in cancer cells. *Cancer Cell* **6**: 129-137.

Thiebaut F, Tsuruo T, Hamada H, Gottesman MM, Pastan I and Willingham MC (1987) Cellular localization of the multidrug resistance gene product P-glycoprotein in normal human tissues. *Proc Natl Acad Sci U S A* **84**: 7735-7738.

Thiebaut F, Tsuruo T, Hamada H, Gottesman MM, Pastan I and Willingham MC (1989) Immunohistochemical localization in normal tissues of different epitopes in the multidrug transport protein P170: evidence for localization in brain capillaries and crossreactivity of one antibody with a muscle protein. *J Histochem Cytochem* **37**: 159-164.

Winter SS, Lovato DM, Khawaja HM, Edwards BS, Steele ID, Young SM, Oprea TI, Sklar LA and Larson RS (2008) High-throughput screening for daunorubicin-mediated drug resistance identifies mometasone furoate as a novel ABCB1-reversal agent. *J Biomol Screen* **13**: 185-193.

Figure legends

Fig. 1. Overview of high-throughput screening data. (A) Hit triage from HTS library screen (10,804 compounds), to compounds that are cytotoxic towards parental KB-3-1 cells (1,362 compounds) to putative P-gp substrates (90 compounds). (B) Summary of percentage of cytotoxic compounds (orange) versus non-toxic compounds (blue), both cumulative and represented in each library screened. (C) Area under the curve (AUC) heatmap of compound activity for screen hits, where red intensity represents magnitude of AUC: deep red is strongest cytotoxicity, and white represents no cytotoxicity.

Fig. 2. Summary of P-gp substrate analysis. (A) Summary of data analysis. For each compound, data is displayed as 'loss of signal from baseline', where -100% represents total cell killing. KB-3-1 cells are sensitive (black), KB-8-5-11 cells are resistant (red) but sensitized when P-gp inhibitor tariquidar is added (blue), top left. To perform HTS data analysis, AUC was determined for the parent and resistant line, and the difference in AUC (termed ΔAUC) is used to identify putative substrates. ΔAUC1 is the difference in AUC in the KB-3-1 (black line) sensitive cells as compared to KB-8-5-11 (red line) resistant cells (top center); ΔAUC2 is the difference in AUC of KB-8-5-11 resistant cells in the absence (red line) and presence (blue line) of tariquidar (top right). Comparison of the AUC for substrates calculated using ΔAUC1 and ΔAUC2, assessing (B) rank order of substrates (where largest ΔAUC is strongest substrate) and (C) orthogonal data generated testing P-gp substrates against HEK cells. (D) Unsupervised clustering of compound activity against parent and resistant lines (with and without tariquidar), where deep red represents greatest cytoxicity.

Fig. 3. Representative examples of known (A-C) and previously unidentified (D-F) substrates of P-gp as determined by the screen.

Fig. 4. Effects of novel P-gp substrates on ATPase activity. The vanadate-sensitive activity of P-gp was determined as outlined in Materials and Methods. Basal P-gp ATPase activity was compared to activity in the presence of 0.1, 1 or 10 μM of the substrates (A) ispinesib, (B) KW-2478, (C) GSK-690693, (D) AT7519 or (E) gedatolisib. Verapamil (F) is shown as a positive control. Graphs depict average values from three independent experiments (error bars +/- SD). Significance was determined by a one-way ANOVA followed by a Dunnet test for multiple comparisons. Asterisks denote significant difference from the control, where $p<0.05$ (*); $p<0.01$ (**).

Fig. 5. Substrate synergy with P-gp inhibitors. Sample combination of elacridar and paclitaxel tested in 10 x 10 dose-response matrices with KB-3-1 (A and B) and KB-8-5-11 (C and D) . A and C, left, percent response of cell viability where red = cell death, black = cell survival. A and C, right, matrix plot in ΔBliss model, magenta = synergy. B and D, dose-response curves extracted from synergy blocks for paclitaxel with increasing concentrations of elacridar. Dose-response curves for (E) tariquidar and (F) elacridar for all substrates tested (listed in Table 2). Values in parentheses are the log of the molar concentration of tariquidar or elacridar needed to achieve maximum cell killing when combined with the noted drugs.

Fig. 6. Inhibition of P-gp- and ABCG2-mediated transport by P-gp substrates. P-gp overexpressing MDR-19 cells (A) or ABCG2 overexpressing R-5 cells (B) were incubated with 0.5 μg/ml rhodamine 123 or 5 μM pheophorbide A, respectively, in the absence or presence a specific inhibitor (3 μM valspodar for P-gp and 10 μM FTC for ABCG2) or 25 μM gedatolisib, KW-2478, ispinesib, GSK-690693, AT9283, or AT7519 for 30 min after which the medium was removed and replaced with substrate-free medium continuing without or with the inhibitor. Cells incubated with substrates alone are shown by the red histogram, cells incubated with the substrate and specific inhibitor are shown by the teal histogram and cells incubated with 25 μM of the test compounds are noted in the key. Results from one of two experiments are shown.

Molecular Pharmacology Fast Forward. Published on September 12, 2019 as DOI: 10.1124/mol.119.115964
This article has not been copyedited and formatted. The final version may differ from this version.

Table 1. Cross resistance profile for novel P-gp substrates in P-gp- or ABCG2-expressing cells

Compound	Structure	GI_{50} pcDNA (μM)	GI_{50} MDR-19 (μM)	RR* P-gp	GI_{50} R-5 (μM)	RR* ABCG2
AT7519	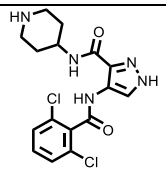	0.61±0.07	66.7±28.2	110	2.3±0.2	4
AT9283	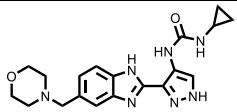	2.7±0.1	34.8±6.8	13	60.8±1.9	22
Ispinesib	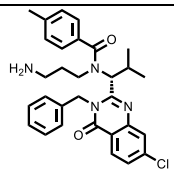	0.044±0.037	2.8±0.5	64	0.14±0.09	3
Gedatolisib	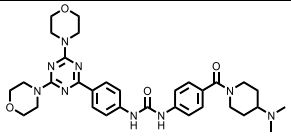	0.028±0.007	47.2±12.8	1672	2.0±0.3	70
GSK-690693	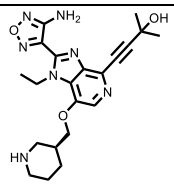	0.19±0.03	56.2±18.8	290	11.6±1.8	60
KW-2478	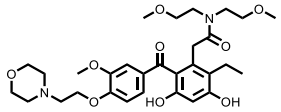	0.48±0.04	129.7±27.5	270	4.5±0.2	9

All compounds were tested in triplicate. Results presented are mean GI_{50} values +/- standard deviation.
*Relative resistance (RR) value is the ratio of the GI_{50} values of P-gp- or ABCG2-expressing cells (MDR-19 or R-5) to the GI_{50} value of pcDNA cells.

Molecular Pharmacology Fast Forward. Published on September 12, 2019 as DOI: 10.1124/mol.119.115964
This article has not been copyedited and formatted. The final version may differ from this version.

Table 2. P-gp substrates tested in combination with elacridar and tariquidar

Compound	**Mechanism of Action**
Mithramycin A	Alcohol Dehydrogenase Inhibitor
Danusertib	Aurora-A/B/C Kinase Inhibitor
Tozasertib	Aurora-A/B/C Kinase Inhibitor
PHA-793887	CDK1,2,3,4,5 Inhibitor
Romidepsin	Histone Deacetylase (HDAC) Inhibitor
JNK-IN-7	JNK inhibitor
PKI-587	mTOR inhibitor
CB 300919	NAMPT inhibitor
AST-487	RET kinase inhibitor
Sepantronium Bromide	Survivin inhibitor
Docetaxel	Tubulin polymerization promoter
Paclitaxel	Tubulin polymerization promoter
Vinorelbine	Tubulin polymerization inhibitor
RO495	Tyk 2 inhibitor
RA-XII	N/A (Natural product)

Molecular Pharmacology Fast Forward. Published on September 12, 2019 as DOI: 10.1124/mol.119.115964
This article has not been copyedited and formatted. The final version may differ from this version.

Figure 1

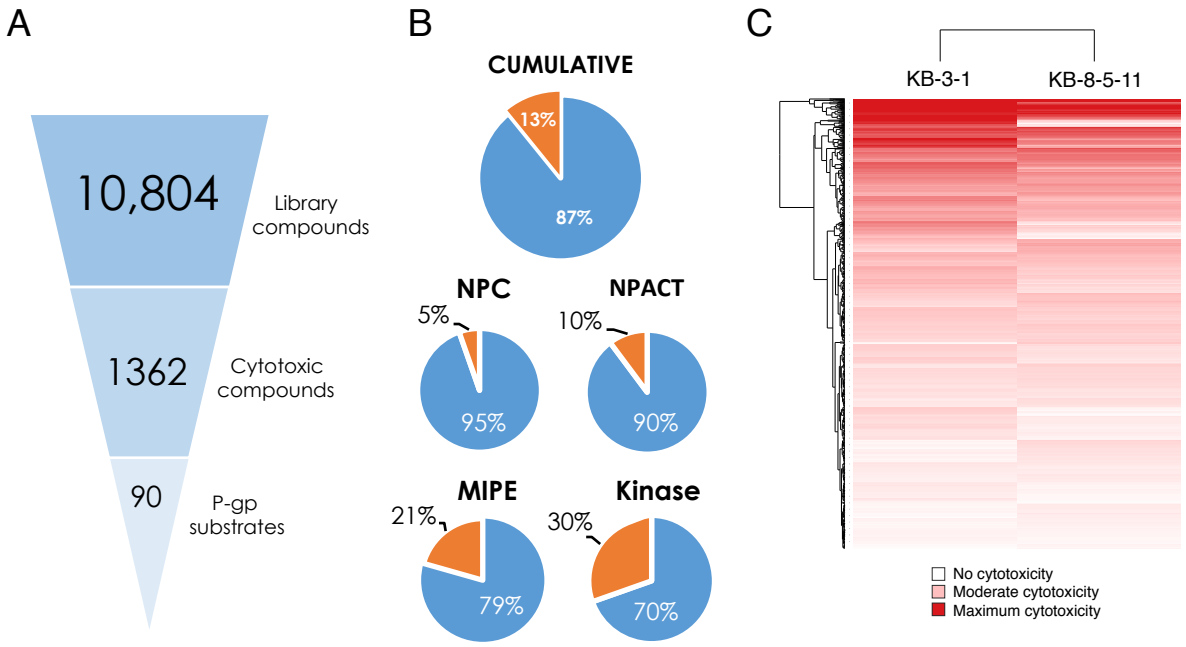

Molecular Pharmacology Fast Forward. Published on September 12, 2019 as DOI: 10.1124/mol.119.115964
This article has not been copyedited and formatted. The final version may differ from this version.

Figure 2

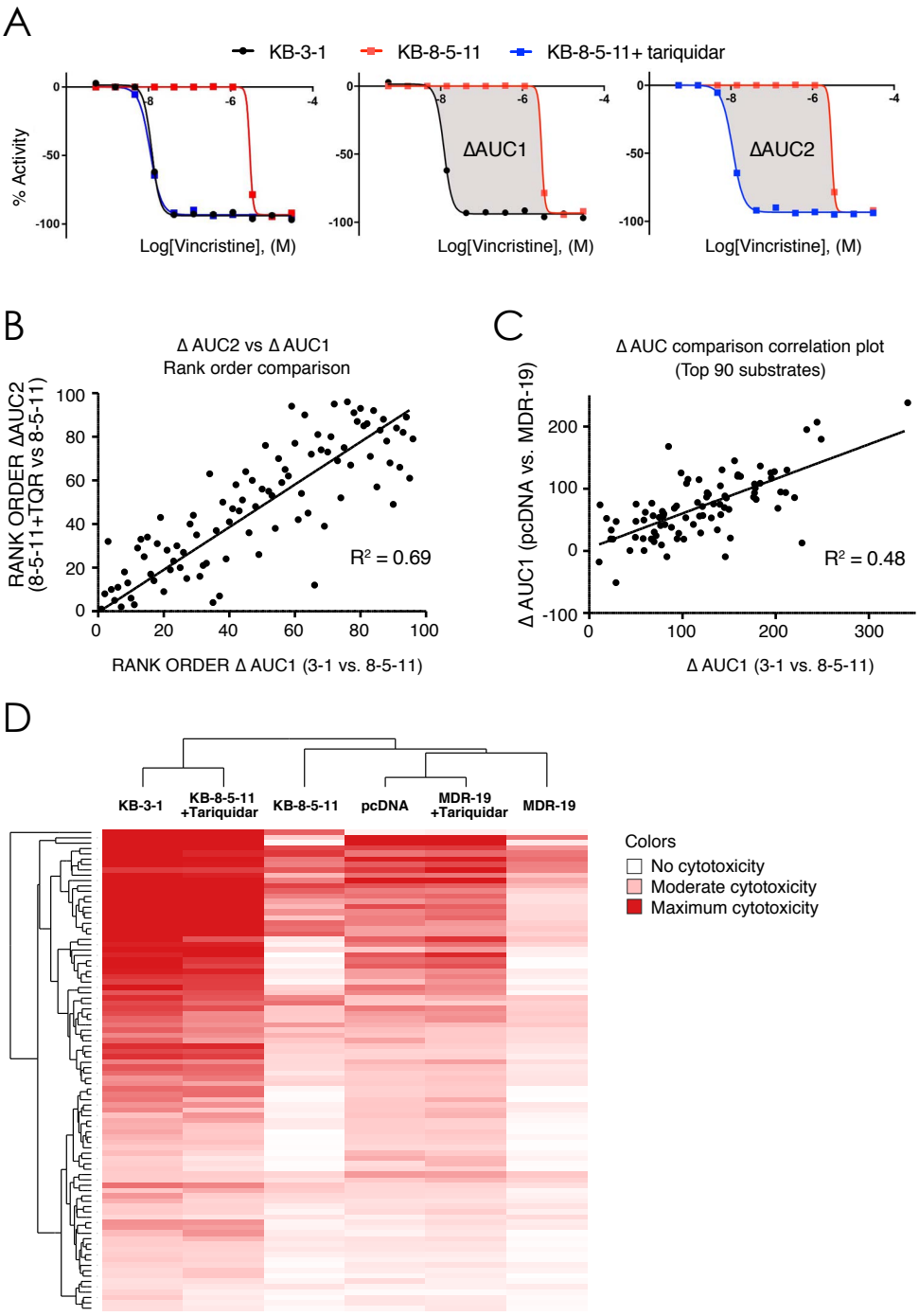

Molecular Pharmacology Fast Forward. Published on September 12, 2019 as DOI: 10.1124/mol.119.115964
This article has not been copyedited and formatted. The final version may differ from this version.

Figure 3

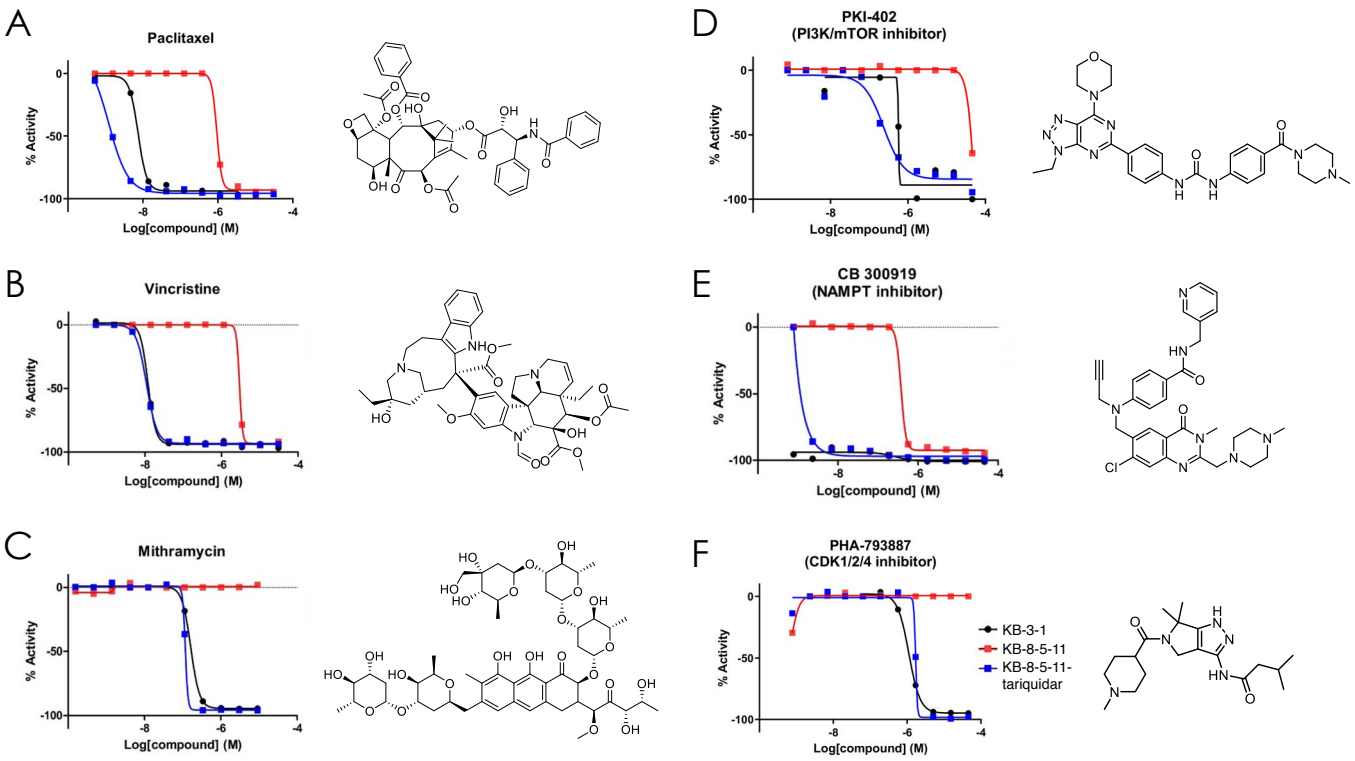

Molecular Pharmacology Fast Forward. Published on September 12, 2019 as DOI: 10.1124/mol.119.115964
This article has not been copyedited and formatted. The final version may differ from this version.

Figure 4

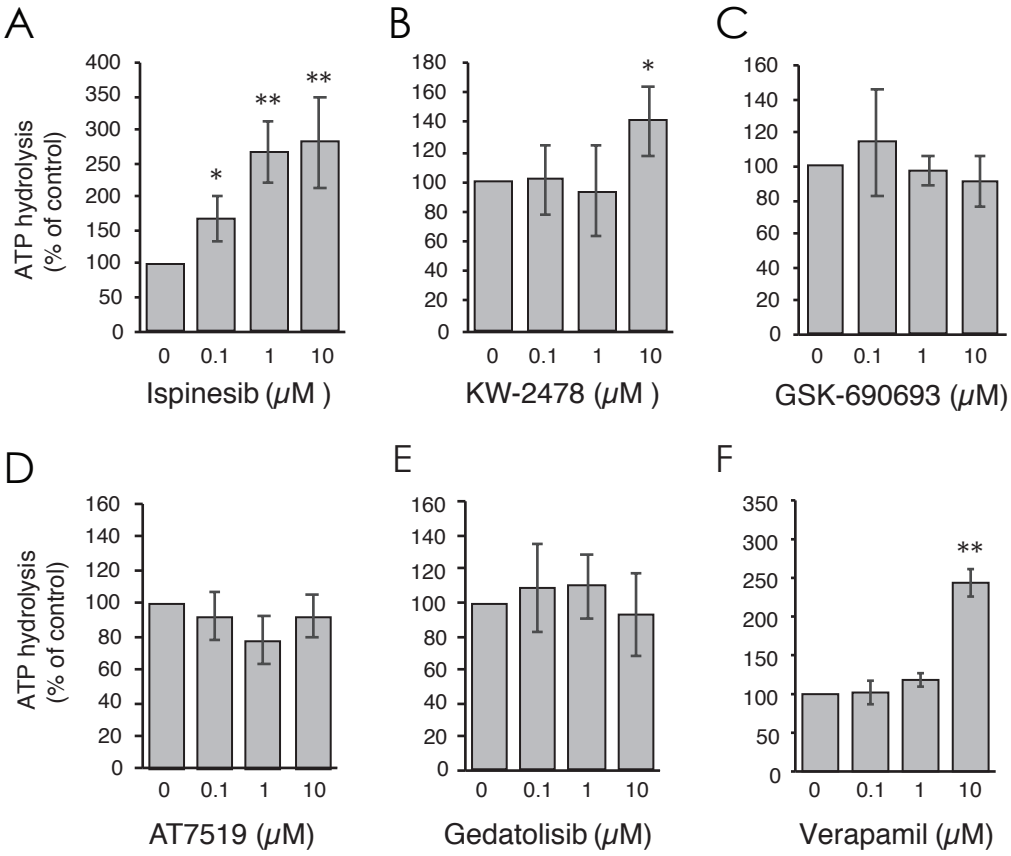

Molecular Pharmacology Fast Forward. Published on September 12, 2019 as DOI: 10.1124/mol.119.115964
This article has not been copyedited and formatted. The final version may differ from this version.

Figure 5

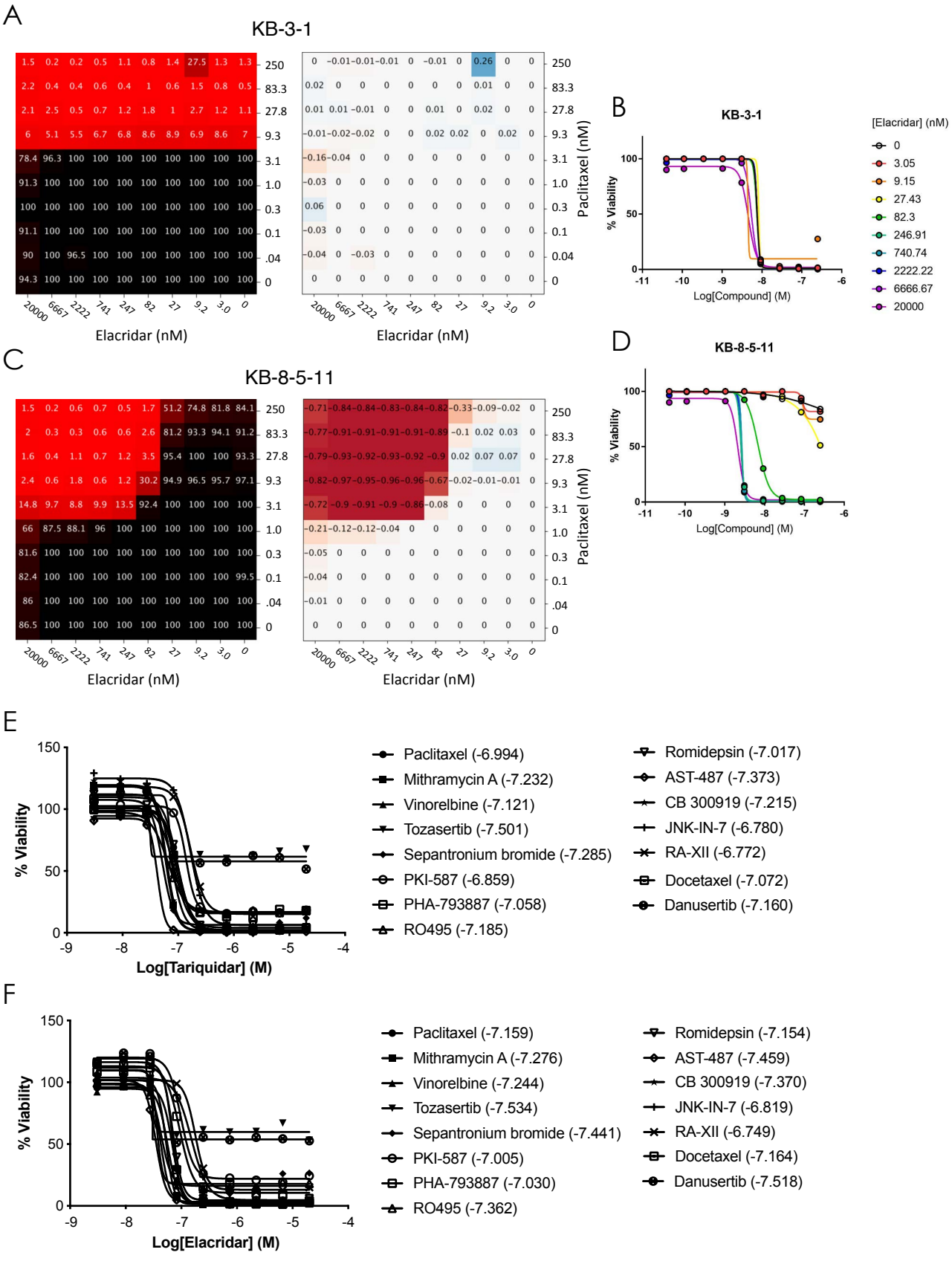

Molecular Pharmacology Fast Forward. Published on September 12, 2019 as DOI: 10.1124/mol.119.115964
This article has not been copyedited and formatted. The final version may differ from this version.

Figure 6

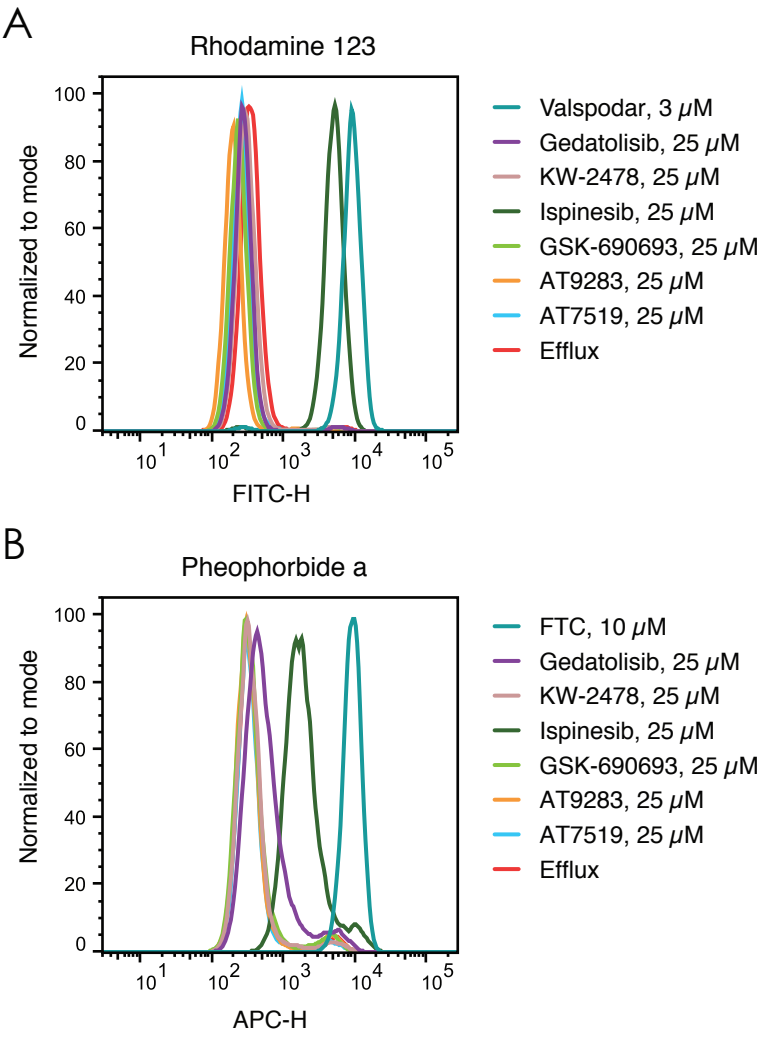

Molecular Pharmacology

A High-Throughput Screen of a Library of Therapeutics Identifies Cytotoxic Substrates of P-glycoprotein

Tobie D. Lee, Olivia W. Lee, Kyle R. Brimacombe, Lu Chen, Rajarshi Guha, Sabrina Lusvarghi, Bethilehem G. Tebase, Carleen Klumpp-Thomas, Robert W. Robey, Suresh V. Ambudkar, Min Shen, Michael M. Gottesman, Matthew D. Hall

Supplementary Table 1. P-gp substrates identified

Sample ID	PMID of P-gp report?	Sample Name	Notes (drug class or mechanism)	Primary MOA	Supplier	Supplier ID	PubChem SID
NCGC00015339	NO	Dequalinium Chloride	Antiseptic	null	Selleck	S4066	144203679
NCGC00016048	YES	Paclitaxel	Cancer	Tubulin depolymerization inhibitor	ChemieTek	CT-0502	363676472
NCGC00017089	12766968	Monensin sodium	Antibiotic (vet)	Polyether Antibiotic	Prestwick Chemical, Inc.	CAS-22373-78-0	144204322
NCGC00018268	16084853	Itraconazole	Antifungal	cytochrome inhibitor	AKos	AKJ-92112	144204405
NCGC00022001	YES	Podophyllotoxin	Warts	Antimitotic Agent; IGF-1R Inhibitors	Prestwick	GPN1A_02E07	144204425
NCGC00024415	YES	Doxorubicin (Adriamycin)	Cancer	DNA Topoisomerase II Inhibitors	SantaCruz Bio	SC-200923	124886890
NCGC00024995	YES	Paclitaxel	Cancer	Tubulin depolymerization inhibitor	Selleck	S1150	363676535
NCGC00091112	NO	Methylrosaniline chloride		TNFR1 (p55/CD120a) Modulator	FLUKA	69710	144204635
NCGC00091387	YES	Ethidium bromide	DNA intercalator	DNA intercalator	SIGMA	E7637	144204674
NCGC00160675	7575681	Carminomycin	Cancer	null	Chemdiv	5181-0657	144205531
NCGC00161419	2521520	Trimetrexate	Cancer	Dihydrofolate Reductase (DHFR) Inhibitors	Tocris	Tocris_2039	144205548
NCGC00161622	YES	Actinomycin D	Cancer	DNA-Directed RNA Polymerase Inhibitor	SIGMA	A1410	144205550
NCGC00161679	NO	MG-132	Proteasome inhibitor	Proteasome Inhibitor	BIOMOL	BIOMOL_PI-102	26755341
NCGC00162423	NO	Mithramycin	Cancer	Alcohol Dehydrogenase Inhibitor	Tocris	Tocris-1489	174007359
NCGC00163424	YES	Tanespimycin	HSP90 inhibitor	Heat Shock Protein 90 (hsp90) Inhibitor	Tocris	1515	144205607
NCGC00163700	YES	Vincristine sulfate	Cancer	Tubulin polymerization inhibitor	BIOMOL	T117	144205620
NCGC00164590	YES	Drospirenone	Contraceptive	Synthetic progesterone	Sequoia	SRP04800d	144205769
NCGC00165966	YES	Vinorelbine	Cancer	Tubulin polymerization inhibitor	SIGMA	V2264	50111727
NCGC00168110	YES	VX-680 (Tozasertib, MK-0457)	Aurora kinase inhibitor	Aurora-A/B/C Kinase Inhibitor	Selleck	S1048	162108261
NCGC00179034	19261919	Pentamidine isethionate	Antimicrobial	PRL Phosphatase Inhibitors	Oakwood	92067	174007138
NCGC00179850	NO	null	Natural product (saponin class)	null	Analyticon	NP-005233	363676977
NCGC00185772	YES	Vindesine sulfate salt	Cancer	Tubulin polymerization inhibitor	Toronto Research	V414550	124896659
NCGC00186273	NO	DMBX-A	partial agonist at neural nicotinic acetylcholine	null	CarsonNewman-SPECS	AT-051/8050095	124897153
NCGC00188123	NO	DMBX-A analog	DMBX-A analog	null	CarsonNewman-SPECS	AT-051/8054374	124898892
NCGC00188128	NO	DMBX-A analog	DMBX-A analog	null	CarsonNewman-SPECS	AT-051/8054424	124898898
NCGC00188382	NO	NCGC00188382-01	ITK inhibitor	ITK inhibitor	NCGCChem	JKJ23-022	162108264
NCGC00188563	NO	null	BIX-01294 analog	null	UNC	UNC00000560A	124899242
NCGC00188564	NO	null	BIX-01294 analog	null	UNC	UNC00000561A	124899243
NCGC00242217	NO	GW 843682X	Plk-1 inhibitor	Polo-like Kinase-1 (Plk-1) Inhibitor	Tocris	2977	137275848
NCGC00242481	NO	AZD7762	Chk1/2 Inhibitor	Chk1/2 Inhibitor	NCGCChem	BTM10-066-C4	363677142
NCGC00242495	NO	PF-431396	FAK inhibitor	Focal Adhesion Kinase (FAK) Inhibitor	SynKinase	PF-562271	124950697
NCGC00242508	YES	Vincristine sulfate	Cancer	Tubulin polymerization inhibitor	ChemPacific	51725	124950707
NCGC00242514	21918035	Sepantronium bromide	Survivin inhibitor	Survivin inhibitor	Selleck	S1130	124950713
NCGC00244256	NO	Lestaurtinib	Jak/Tyk/Flt inhibitor	Jak/Tyk/Flt inhibitor	Alfa Aesar	J60602	174006757
NCGC00249613	27118406	Carfilzomib (PR-171)	Cancer	Proteasome Inhibitor	Selleck	S2853	144206630
NCGC00250398	NO	PKI-587	mTOR inhibitor	mTOR inhibitor	Selleck	S2628_CM1	137275899
NCGC00253438	23593196	BI-2536	Plk-1 inhibitor	Polo-like Kinase-1 (Plk-1) Inhibitor	Selleck	S1109	137275913
NCGC00253463	NO	NCGC00253463-01	Chk1/2 inhibitor	Chk1/2 inhibitor	NCGCChem	BTM10-066-A5	137275915
NCGC00263087	26412161	Volasertib (BI 6727)	Plk-1 inhibitor	Polo-like Kinase-1 (Plk-1) Inhibitor	ChemAxon	Axon 1473	363677196
NCGC00263089	23315030	AZD-1152-HQPA	Aurora kinase inhibitor	Aurora-A/B Inhibitor	ChemAxon	Axon 1580	363677197
NCGC00263091	NO	AT7519	CDK 1 & 2 inhibitor	CDK 1 & 2 inhibitor	Selleck	S1524	137275934
NCGC00263112	25192198	GSK461364	Plk-1 inhibitor	Polo-like Kinase-1 (Plk-1) Inhibitor	MedChem Express	HY-50877_CM1	137275956
NCGC00263117	NO	Panobinostat (LBH589)	HDAC inhibitor	Histone Deacetylase (HDAC) Inhibitor	ChemAxon	Axon 1548	363677212
NCGC00263132	NO	PF-477736	Chk1 Inhibitor	Chk1 Inhibitor	ChemAxon	Axon 1379	363677219
NCGC00263136	NO	Pracinostat	HDAC inhibitor	Histone Deacetylase (HDAC) 1/2 Inhibitor	ChemAxon	Axon 1777	363677222
NCGC00263146	NO	SR-3306	JNK 1/2/3 Inhibitor	JNK 1/2/3 Inhibitor	EMD Chemicals	420147	137275990
NCGC00263167	27517323	SNS-032	CDK2,7,9 Inhibitor	CDK2,7,9 Inhibitor	Selleck	S1145	174007077
NCGC00263168	NO	PHA-793887	CDK1,2,3,4,5 Inhibitor	CDK1,2,3,4,5 Inhibitor	Selleck	S1487	363677240
NCGC00263174	23593196	Ispinesib	Kinesin-Like Spindle Protein Inhibitor	Kinesin-Like Spindle Protein Inhibitor	Selleck	S1452	137276018
NCGC00263177	25450670	CUDC-101	HDAC/EGFR inhibitor	EGFR (HER1; erbB1) inhibitor	ChemieTek	CT-CU101	363677246
NCGC00263181	NO	GSK-690693	Akt1/2/3 Inhibitor	Akt1/2/3 Inhibitor	Selleck	S1113	137276025
NCGC00263183	NO	MK-1775	Wee1 Kinase Inhibitor	Wee1 Kinase Inhibitor	Selleck	S1525	363677250
NCGC00263200	NO	RO495	Tyk 2 inhibitor	Tyk 2 inhibitor	SynKinase	SYN-1128	137276044
NCGC00263220	YES	Romidepsin	HDAC inhibitor	Histone Deacetylase (HDAC) Inhibitor	Selleck	S3020	174006359
NCGC00263223	NO	CAY10626	PI3Kalpha inhibitor	PI3Kalpha inhibitor	Cayman	13838	137276067
NCGC00263265	NO	ASR-isobudimer-SO2Ph-4-CH2OC(	artemesinin analogue	artemesinin analogue	JohnsHopkins	mer-SO2Ph-4-CH2OC(O	137276084
NCGC00263270	NO	BTM-2C-dimer allyl oxime	artemesinin analogue	artemesinin analogue	JohnsHopkins	3TM-2C-dimer allyl oxime	137276086
NCGC00345784	23524533	PF-3758309	PAK4 inhibitor	p21-Activated Kinase 4 (PAK4) Inhibitors	Selleck	S7094	174006763
NCGC00345799	22235146	Oprozomib	Proteasome Inhibitor	Proteasome Inhibitor	ChemieTek	CT-OPRO	174006320
NCGC00345815	NO	MG-115	Proteasome Inhibitor	Proteasome Inhibitor	Peptides Intl	IAT-3170-v	174006366
NCGC00346469	NO	Delanzomib	Proteasome Inhibitor	Proteasome Inhibitor	Ontario Chemicals	C3599	363677416

NCGC00346493	NO	AT9283	Aurora kinase inhibitor	Aurora-A/B Inhibitor	MedChem Express	HY-50514	363677426
NCGC00346526	NO	PHA-680632	Aurora kinase inhibitor	Aurora-A/B/c Inhibitor	Selleck	S1454	363677441
NCGC00346571	NO	SB-743921	Kinesin-Like Spindle Protein Inhibitor	Kinesin-Like Spindle Protein Inhibitor	Selleck	S2182	174007342
NCGC00346645	23358665	TAK-901	Aurora kinase inhibitor	Aurora-A/B Inhibitor	Selleck	S2718	174006378
NCGC00346649	NO	PKI-402	PI3K Inhibitor	PI3K Inhibitor	Selleck	S2739	174006456
NCGC00346685	NO	KW-2478	HSP90 inhibitor	Heat Shock Protein 90 (hsp90) Inhibitor	Selleck	S2685	174007110
NCGC00346954	NO	TCS-2312	Chk1 Inhibitor	Chk1 Inhibitor	Tocris	3038	174007019
NCGC00346964	NO	WZ3105	FLT3 inhibitor	FLT3 Inhibitor	LINCS	HMSL10084	174006425
NCGC00346966	NO	XMD13-2	RIPK1 inhibitor	Receptor-interacting serine/threonine-protein kina	LINCS	HMSL10088	174006754
NCGC00347665	NO	null	Natural product	null	Analyticon	NP-008036	363677661
NCGC00354729	NO	AST-487	RET kinase inhibitor	RET kinase inhibitor	SynKinase	SYN-1210	363677788
NCGC00370777	NO	PF-05212384 (PKI-587)	PI3K Inhibitor	PI3K Inhibitor	APExBIO	B2179	363677849
NCGC00378821	NO	CB 300919	NAMPT inhibitor	NAMPT inhibitor	MedChem Express	HY-14375	363678220
NCGC00379020	NO	JNK-IN-7	JNK inhibitor	JNK inhibitor	APExBIO	A3519	363678319
NCGC00380703	NO	Destruxin	Natural product	null	Analyticon	NP-007389	363678720
NCGC00380800	NO	Trienomycin A	Natural product	null	Analyticon	NP-012065	363678788
NCGC00384584	NO	Avenacoside A	Natural product	null	Analyticon	NP-001834	363679260
NCGC00384689	NO	Ageratoside B2	Natural product	null	Analyticon	NP-007564	363679313
NCGC00384826	NO	RA-XII	Natural product	null	Analyticon	NP-018672	363679380
NCGC00384923	NO	Natural product	Natural product	null	Analyticon	NP-004783	363679442
NCGC00385268	NO	Toosendanin	Natural product	null	Analyticon	NP-005159	363679628
NCGC00386325	YES	Vinorelbine Tartrate	Tubulin polymerization inhibitor	Tubulin polymerization inhibitor	Selleck	S4269	363680211
NCGC00386339	YES	Vincristine	Tubulin polymerization inhibitor	Tubulin polymerization inhibitor	Selleck	S1241	363680221
NCGC00386371	NO	Ro3280	PLK1 inhibitor	PLK1 inhibitor	Glixx	GLXC-06183	363680242
NCGC00387092	NO	PF 429242	Proteasome inhibitor	Proteasome inhibitor	Adooq	A11230	363680540
NCGC00387828	YES	Docetaxel	Tubulin polymerization inhibitor	Tubulin depolymerization inhibitor	ChemieTek	CT-0521	363680684
NCGC00389696	20935223	Danusertib (PHA-739358)	Aurora kinase inhibitor	Aurora-A/B/C Kinase Inhibitor	APExBIO	A4116	363680831
NCGC00390686	NO	NBD-557	HIV1 entry inhibitor	HIV1 entry inhibitor	MedChem Express	HY-76649	363680970
NCGC00402294	NO	Mps1-IN-3	MPS1 inhibitor	MPS1 inhibitor	Glixx	GLXC-03888	363681017